sciendo

Research Note • DOI: 10.2478/gsr-2022-0001 GSR • 10 • 2022 • 1–9

Gravitational and Space Research

Nonlinear Agglomeration of Bimodal Colloids under Microgravity

Adam J. Cecil[1], John E. Payne[2], Luke T. Hawtrey[1], Ben King[2], Gerold A. Willing[1], Stuart J. Williams[2]

[1]Department of Chemical Engineering, University of Louisville; [2]Department of Mechanical Engineering, University of Louisville

Abstract

A study of like-charged, bimodal colloidal suspensions was conducted in microgravity aboard the International Space Station as part of NASA's Advanced Colloids Experiments-Heated-2 (ACE-H-2) experiments. Samples comprised of silsesquioxane microparticles (600 nm) and zirconia nanoparticles (5–15 nm) in 1.5 pH nitric acid were mixed and allowed to agglomerate over time while being imaged with NASA's Light Microscopy Module (LMM). The samples contained 1% of microparticles with varying concentrations of nanoparticles in 0.1%, 0.055%, and 0.01% by volume. Digital images were captured periodically by the LMM over 12 days. Image analysis, including cluster size and distribution, was performed in Python using the "Colloidspy" package. The study found that cluster size had increased over time in at least seven of nine samples, but two samples exhibited nonlinear growth rates, while others showed very slow growth with cluster sizes two orders of magnitude greater than the free microparticles. We hypothesize that all samples experienced nonlinear growth, but early transient effects after mixing were missed due to timing limitations in image acquisition. Transport limitations of clusters in these systems may have dominated agglomeration behavior in microgravity, despite the samples being thermodynamically unstable, but more study is required.

Keywords

Bimodal • Colloids • Colloidspy • Nonlinear • Stabilization • Transport

INTRODUCTION

Colloid Science

Colloidal suspensions are discrete mixtures of two or more materials that interact to form two or more immiscible phases. One phase must be continuous while the other phases are discontinuous and remain stabilized within the continuous phase. The phases may be solid, liquid, or gas, thus creating many variations. Consumer products based on colloidal systems include, but are not limited to, paints (Tadros, 2010), ceramics (Lewis, 2000), foams (Kontogeorgis and Kiil, 2016), personal care products (Tadros, 2008), and pharmaceutical formulations (Sinko and Martin, 2006). These examples, among others, require that the dispersed phase remain stable over the lifetime of the product, in which the solution does not separate or form agglomerates. Thus, fundamental investigations into long-term colloidal stability are applicable toward improved shelf-life and consistent performance of everyday products.

Long-term colloidal stability depends on a series of carefully balanced interaction forces (Lyklema, 2000). While the mechanisms for stabilization can vary, most require balancing the attractive and repulsive forces within the system (Grządka, 2015). The attractive forces within a colloidal suspension vary from system to system, but the main sources of attraction are from van der Waals forces. Van der Waals forces, which include London dispersion forces, dipole-dipole interactions, and dipole-induced dipole interactions, tend to only act at close distances of <10 nm, and decrease in magnitude with increasing distance (Hiemenz, 1972; Ottewill, 1997). Since they are predominantly attractive, they must be counteracted by repulsive forces to maintain system stability (Israelachvili, 2011).

The source of repulsive forces in colloids also varies between systems. One of the simplest is electrostatic repulsion, in which particles of like charge experience Coulombic repulsion, thus counteracting the attractive van der Waals forces (Walz and Sharma, 1994). Of particular importance to this study is charge regulation, an electrostatic stabilization method (Bakhshandeh et al., 2020; Ninham and Parsegian, 1971). Charge regulation relies on a charged double-layer effect to repel other particles: charged microparticles suspended in an electrolyte adsorb to the particle surface creating an ion layer, and counter-ions gather to create a second ion layer suspended just outside the inner layer. If the electrical potential between the double layers of two particles is greater than the attractive van der Waals forces present between them, the system will remain stable (Ottewill, 1997).

Of recent interest, nanoparticle haloing (NPH) can also be utilized to effectively counter the attractive van der Waals forces.

†Corresponding author: Stuart J. Williams
E-mail: stuart.williams@louisville.edu

This colloidal stabilization technique manipulates properties of particles in a binary mixture that was first described by Tohver et al. (2001). The size of one population of particles is on the order of micrometers and the other on the order of nanometers. The zeta potential of the larger particles is set at its isoelectric point, in which the only intermolecular forces acting upon the microparticles are van der Waals forces, while the nanoparticles are highly charged. At particular proportions of nano- and microparticles, nanoparticles both adhere to and form halos around the microparticles to create an effective electrostatic repulsive barrier to screen the van der Waals forces and stabilize the suspension (Moradi et al., 2019a). At this state, the suspension is metastable and forms an ordered crystalline solid phase.

Zeta Potential

The surface charge of a particle submerged in a colloidal solution creates two parallel layers of alternating positive and negative ions, referred to as the electric double layer. The first layer is due to the chemical interactions of the surface charge adsorbing ions of the opposite charge of the surface charge. The second layer, called the Stern Layer, is created due to Coulombic forces of the first layer. The ions within this Stern Layer are not as strongly bonded as the first layer but have the same charge as the particle's surface. The zeta potential is found on the surface of this double layer, called the slipping plane, determined by the difference in potential of the medium and potential of the double layer attached to the particle (Hunter et al., 2013). Zeta potential on an absolute scale is directly proportional to the stability of the colloidal solution – a greater magnitude of zeta potential enhances colloid stability, preventing particle aggregation. For example, zeta potentials near ±15 mV may experience rapid aggregation, whereas zeta potentials in the range of ±40–60 mV could remain stable long-term, depending on the interactions present and respective sizes of the colloidal particles (Kumar and Dixit, 2017).

Bimodal Systems

Where NPH requires negligibly charged microparticles and highly charged nanoparticles within a very narrow concentration range, bimodal systems only require that the two particles be of different sizes. One of the earliest models of bimodal colloids was pioneered by Asakura and Oosawa (1958) with their introduction of the depletion region – spaces between large particles small enough to exclude smaller particles are subjected to osmotic pressure pushing the large particles together, due to the entropic tendency for the small particles to reduce the concentration difference between the interparticle space and the bulk. Later models included a wide range of effects due to variables such as dissymmetrical species, concentration differences, long-range electrostatics, polydispersity, polymers, and more (Chatterjee and Schweizer, 1998a, 1998b; Chu et al., 1996; Shah et al., 2003; Walz and Sharma, 1994; Weight and Denton, 2018). In addition to thermodynamic metrics such as potential energy balances, changes in enthalpy, and partition functions, other options have been explored for controlling colloidal stability. A team of researchers from University of Washington exploring the effects of altering particle ratios were able to limit particle transport enough to temporarily halt the agglomeration of thermodynamically unstable systems (Liu et al., 1991; Yasrebi et al., 1991). Another group in 2016 found that attractive and unstable systems could remain stable as long as the entropy of mixing resulted in strong enough negative free-energy to discourage phase separation (Mo et al., 2016).

The colloidal suspension observed in this study is a suspension of like-charged particles at a nanoparticle–microparticle size ratio of 60:1, microparticle volume fraction of 10^{-2}, and nanoparticle volume fractions between 10^{-3} and 10^{-4}. Experiments performed by Moradi et al. confirmed that only sub-monolayer adsorption of nanoparticles occurs within this volume fraction and size ratio for NPH systems. The significant difference between this system and NPH systems is that the microparticles in this system are charged. Since the micro- and nanoparticles are like-charged, electrostatic interactions between particles disfavors adsorption even more strongly than in NPH systems. Consequently, there are free nanoparticles in solution to contribute to depletion interactions and cause phase separation.

Cluster Size Analysis

Cluster size analysis is a basic 2D mathematical model used to describe a binary image as a series of aggregated clumps. The model developed for this analysis uses a local thresholding algorithm coupled with a watershed algorithm to convert the images to a binary format in which white pixels represent particle agglomerates. From the binary image, connected regions of white pixels are identified as clusters. Use of local as opposed to global thresholding minimizes the sensitivity of such size analysis on specific thresholding parameters.

MATERIALS AND METHODS

Light Microscopy Module (LMM)

Particles that can be visualized using a standard microscope (diameters >1 μm) typically sediment within seconds or minutes, unless their density is matched with the suspending medium (Wiederseiner et al., 2011). Gravity hinders the observation of fundamental physical mechanisms guiding particle interactions, including identifying particularly the self-assembly of such structures. Thus, over the past few decades

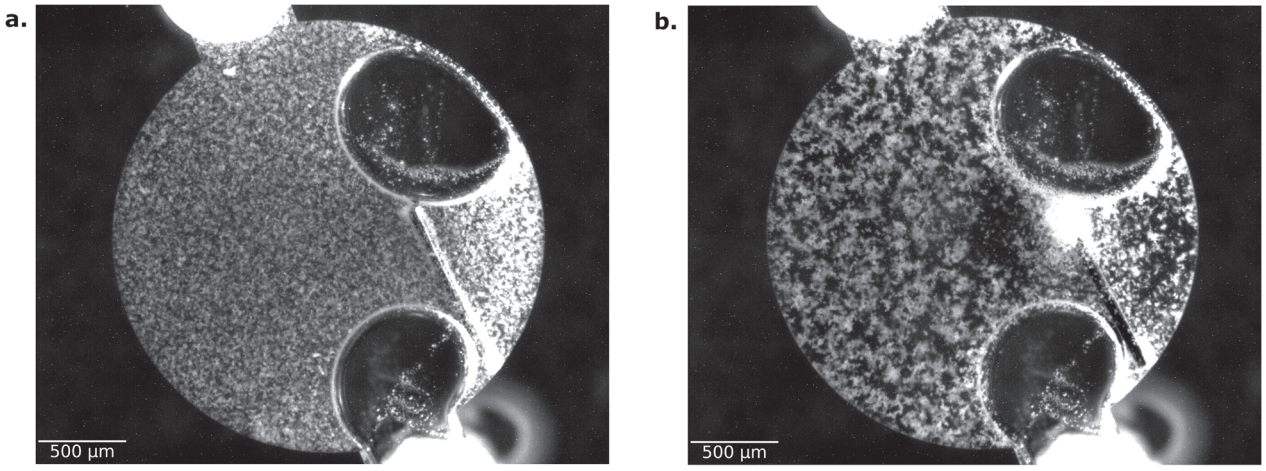


Figure 1. Images of a low-concentration nanoparticle (0.01% ZrO_2) well (A) on the first day after being mixed and (B) 12 days later.

there has been a thrust in microgravity colloid research on the ISS (Ansari et al., 1999; Swan et al., 2012; Veen et al., 2012). In response to the growing interest, NASA established the Advanced Colloids Experiment (ACE) program to coordinate future efforts on the ISS. Specifically, this study is part of the Advanced Colloids Experiments-Heated-2 (ACE-H-2) series of experiments. The Light Microscopy Module (LMM) was developed to visualize the colloidal interactions in this experiment. The LMM on the ISS is an automated microscope that has been built in stages (Lant and Resnick, 2000). It allows flexible imaging (e.g., bright field, dark field, phase contrast, confocal microscopy) for physical and biological experiments and can be commanded from the ground. The LMM accommodates sample changeout and fluid containment and includes a glovebox for on-orbit sample manipulation. This unique capability can support a large set of experiments that require visual imaging of a small test sample.

Sample Preparation

For our experiments forming part of the ACE-H-2, benzyl chloride functionalized silsesquioxane microspheres (600 nm, synthesized using the method described by Moradi et al. (2019b) at 0.01 volume fraction) were suspended along with three different concentrations (0.1%, 0.05%, 0.01% by volume) of charged zirconia (ZrO_2) nanoparticles (from Nyacol Nano Technologies Inc., Ashland, MA, USA). The manufacturer-reported diameter of the nanoparticles was 10 nm, with a Gaussian size distribution in the range of 5–15 nm. The media was an aqueous solution of nitric acid (Fischer Scientific, Pittsburgh, PA, USA) set at 1.5 pH, intended to reach the silsesquioxane microparticles' isoelectric point. According to NPH literature, these volume fractions provide the greatest stability range while allowing visibility of individual clusters via confocal microscopy (Tohver et al., 2001). However, later testing found that the functionalized silsesquioxane's isoelectric point was not equal to that of silica as advertised, but 2.8 pH, making this system bimodal, and not a NPH system (Moradi et al., 2019b). Fifteen samples (five of each nanoparticle concentration) were sealed in 2.5 mm diameter, 0.2 mm depth disc-shaped circular wells with a stainless-steel mini-rod, as shown in Figure 1. Our samples launched on Atlas V OA-4 on December 6, 2015.

Experimental Method

Prior to observation, an astronaut manually mixed each sample well by agitating the mini-rod using a magnetic wand for 2 minutes before loading the sample into the LMM. Samples were illuminated from the side to induce scattering since the particles were not fluorescent. The sample wells were observed over the course of 12 days at an approximate rate of 10 images per day per well. The image files were labeled with a timestamp and magnification level, stored in the station's computers, and analyzed by methods as described later in the paper. Not all of the wells were analyzed, as some were compromised (excessive bubble formation, inadequate mixing, etc.). Additionally, an undocumented time of long as 5–8 h passed between mixing and the start of imaging. Nine of the fifteen uncompromised wells were analyzed: three low-concentration wells at 0.01% ZrO_2, three intermediate-concentration wells at 0.055% ZrO_2, and three high-concentration wells at 0.1% ZrO_2. Figure 1 shows one well at the beginning and end of imaging. The two large circles inside of the well are air bubbles introduced during sample transport to the ISS and were unavoidable.

Python

Python (Python, 2021) is a high-level programming language used in a wide range of scientific applications, and is most commonly coupled with external, open-source Python libraries. Colloidspy (Cecil, 2021), an image analysis package, was developed to analyze the images in this study. The analysis methods are a simple Python implementation of methods used by ImageJ for particle detection (Papadopulos et al., 2007), with the notable addition of local thresholding to minimize threshold sensitivity.

Colloidspy (Cecil, 2021) utilizes *NumPy* (Harris et al., 2020), *SciPy* (Virtanen et al., 2020), *pandas* (McKinney, 2010), *scikit image* (Van Der Walt et al., 2014), and *OpenCV* (Bradski, 2000) Python packages. Package construction, design, and assumptions are discussed in detail in the following thesis and corresponding GitHub page: Cecil (2021).

Cluster Size Analysis

A region of interest (ROI) was selected for a series of images. All the images in the series were cropped to that ROI; then a local thresholding algorithm was applied to convert the image to binary, leaving only clusters in the frame. The images were cleaned to remove single-pixel noise, and a watershed and contour detection algorithm was applied to separate discrete clusters that appeared to be touching in the image. Finally, individual cluster data, including area, perimeter, convexity defects, and circularity were extracted and exported for further analysis. A visual example of this analysis progression is shown in Figure 2. As another visual aid, Figure 3 shows sample images of average particle sizes of 800 μm^2, 1100 μm^2, and 1400 μm^2.

RESULTS

The average cluster area over settling time for each sample, separated by zirconia nanoparticle concentration, are shown in Figures 4–6. Samples of 0.01% ZrO_2 are designated with “A#”, samples with 0.055% ZrO_2 are designated with “B#”, and finally, the 0.1% ZrO_2 samples with “C#”. Regression curves are shown to guide the eye and do not imply a formal agglomeration model proposal. Error bars indicating the 95% confidence intervals for the Poisson mean particle sizes are included but are not easily visible as they are three orders of magnitude smaller than the datapoints.

Cluster growth rates in samples A1–3 were nearly identical, as expected with physically identical systems. The early datapoints of A1 resemble the tail-end of a nonlinear cluster growth period, quickly reaching a growth rate in accordance with the other samples. In contrast, strong nonlinear cluster growth was observed in samples B2–3. Samples C1–3 are almost identical in behavior to samples A1–3: C1 exhibits

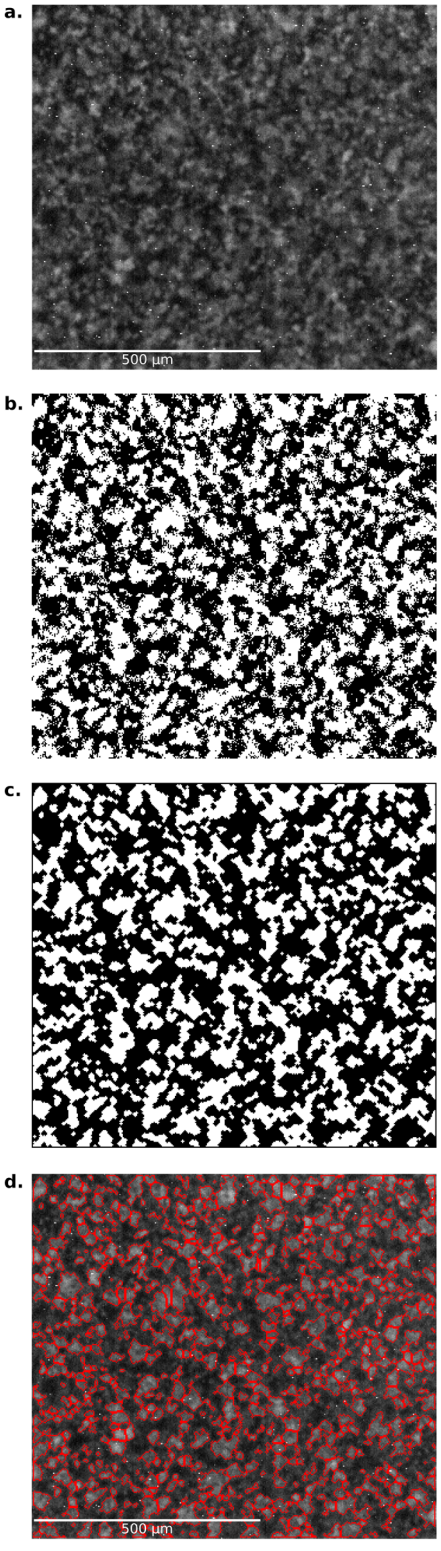


Figure 2. Progression of cluster size analysis. (A) Cropped image, (B) binarized, (C) cleaned, (D) – particle outlines drawn in red over original cropped image.

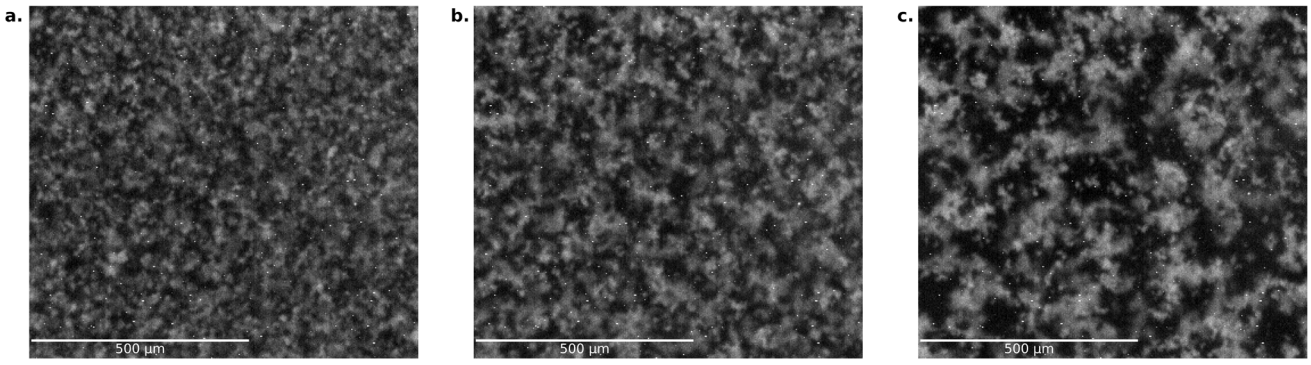


Figure 3. (A) Average cluster size of 800 µm^2; (B) average cluster size of 1,100 µm^2; (C) average cluster size of 1,400 µm^2.

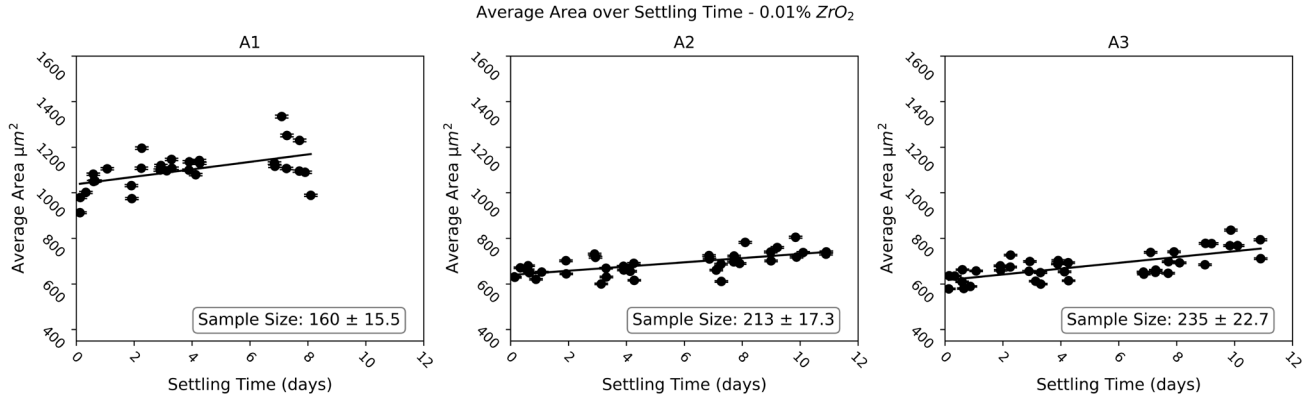


Figure 4. Average cluster versus days since mixed for 0.01% ZrO_2 concentration.

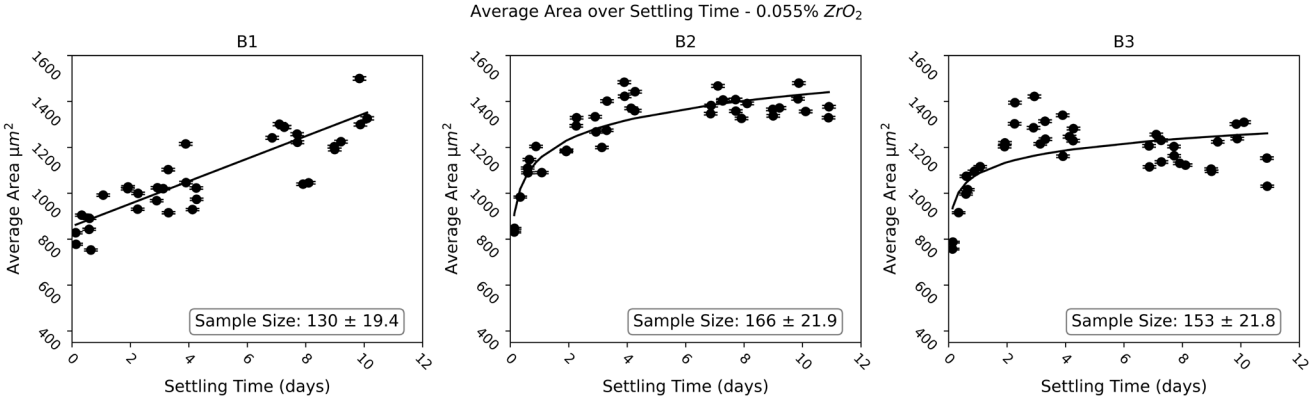


Figure 5. Average cluster size versus days since mixed for 0.055% ZrO_2 concentration.

interesting, perhaps nonlinear behavior at the beginning of its growth, stabilizing to a slow growth rate resembling that of the other samples. In all cases, beginning and final cluster sizes are two orders of magnitude higher than the projected area of a single silsesquioxane particle, indicating that large amounts of agglomeration had already occurred by the time the first images were taken. Indeed, to obtain the lowest cluster sizes observed at the beginning of imaging within 8 h, the upper bound of undocumented time, the agglomeration rate would need to be 100× faster than the fastest linear-region agglomeration rate observed from these images. As expected, ground control experiments showed complete

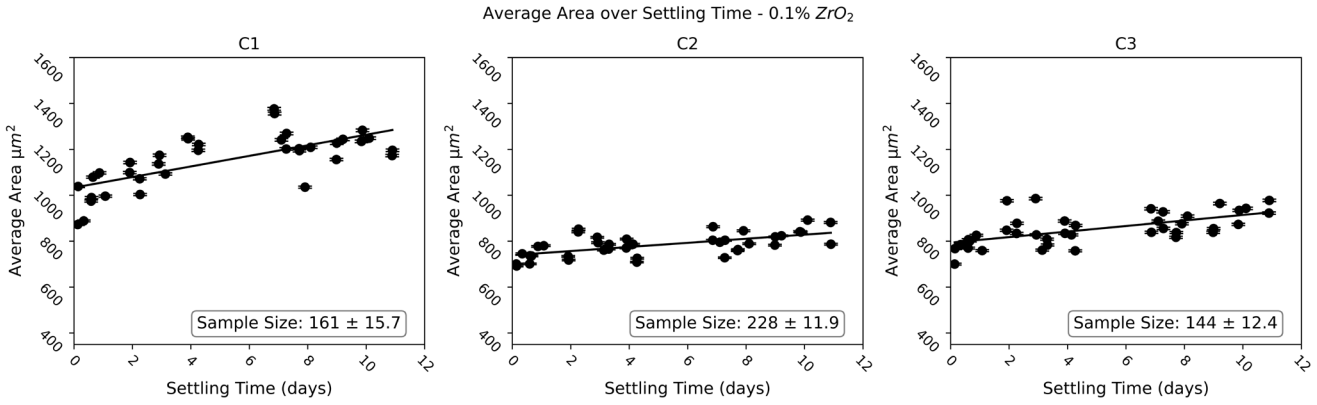


Figure 6. Average cluster size versus days since mixed for 0.1% ZrO_2 concentration.

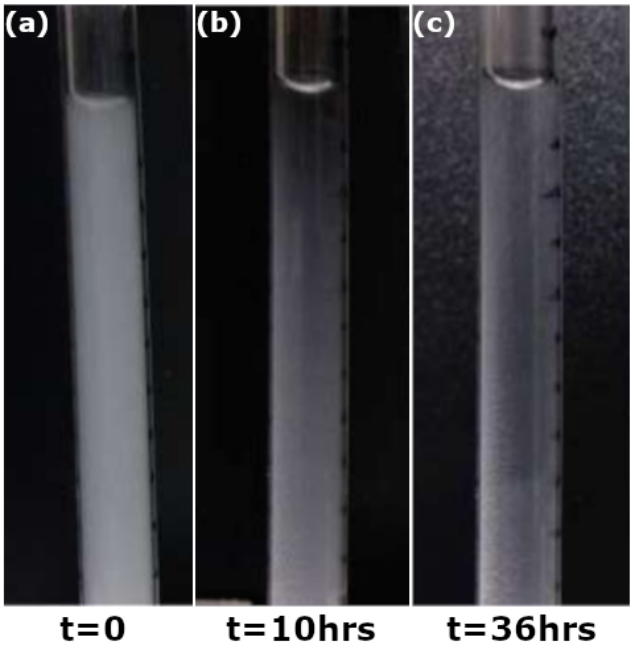


Figure 7. Ground control sedimentation experiment of 0.01% ZrO_2 at 0 h (A), 10 h (B), and 36 h (C).

sedimentation of these colloidal systems within 10 h, as shown in Figure 7 (Moradi et al., 2017). Similar in-depth testing and image analysis was not conducted as agglomeration behavior in gravity is tangential to the focus of this study.

DISCUSSION

As shown in Figure 5, the cluster growth behavior for samples B1–3 is drastically different from that of the other samples. One notable possibility for this difference in observed behavior is that imaging of these samples could have begun earlier than in other samples, revealing a rapid growth phase present in all samples. Additionally, cluster growth may be slower at this intermediate nanoparticle concentration, stretching existing nonlinear behavior out over time. Due to experimental limitations in the ISS, an undocumented time as large as 5–8 h had passed between sample mixing and start of imaging. Observing the similarity in final cluster growth rates across all samples, it is highly possible that the initial rapid growth observed in samples B1–3 is common among all samples but occurred before the start of imaging in the samples that appear linear. This hypothesis is supported by slight potential nonlinearity at the beginnings of samples A1 and C1, as well as the large magnitude of cluster sizes among all samples compared to free silsesquioxane microparticles. Alternatively, another explanation could be that there is simply more nonlinear behavior at 0.055% ZrO_2 than at other concentrations, but no mention of this sort of behavior has been found in literature near the experimental conditions tested.

Theory developed by Walz and Sharma (1994) predicts that bimodal colloidal suspensions with nanoparticle concentrations <~0.5% (size ratio 1,000:1) would exhibit only attractive interparticle forces, indicating that unbounded linear agglomeration should be seen in all samples tested in this study. While the size asymmetry in this study was smaller than that used by Walz and Sharma, eventual near-stabilization of these systems was still unexpected, particularly considering that terrestrial samples destabilized quickly. Supporting theory developed by Chu et al. (1996) predicted that decreasing size ratio should strongly decrease repulsive interparticle forces and increase the depth of the potential well within the depletion region, causing a net increase in both agglomeration rate and strength. This theory coupled with that by Walz and Sharma is contradictory to the observations from this study.

Chu et al.'s predictions also included that increasing secondary phase concentration should increase agglomeration rate (Chu et al., 1996). In this study, the secondary phase (ZrO_2) concentration was increased in three steps (samples A, B, and C, respectively). Following this theory, the agglomeration rates should increase linearly with both time and increased nanoparticle concentration. In contrast, all samples tested showed roughly equal, slow final agglomeration rates, approaching stabilization.

Rapid growth phases followed by near-stabilization in the intermediate-concentration samples (B1–3) suggest that forces other than thermodynamics may be dominating the system in microgravity conditions. Several studies have found that high concentrations of the secondary phase can cause quasi-stabilization by inhibiting movement of the primary phase (Liu et al., 1991; Yasrebi et al., 1991). Along a similar idea, we hypothesize that without buoyancy from gravitational forces to continuously reduce interparticle space, the thermal energy of large clusters may not be enough to sustain constant agglomeration that would be observed in a gravity environment. As small clusters and single particles agglomerate together, regions immediately surrounding these clusters slowly deplete of the primary phase, increasing the transport required to continue agglomeration. As the distance between clusters increases, attractive thermodynamic forces decrease in strength (Chu et al., 1996; Walz and Sharma, 1994), leaving transport to dominate system stabilization.

Further study of the interplay between thermodynamic and transport stabilization of colloids in microgravity is required to confirm this hypothesis. Specifically, particle tracking could be a useful tool; by the hypothesis from this study, the mean free path of clusters should decrease as cluster size increases, and particle movements should slow enough that cluster do not significantly interact with other clusters on their random-walks after the initial growth phase. Finally, direct observation of the transient effects of bimodal colloids in microgravity immediately after mixing should be pursued in future studies.

CONCLUSIONS

In this experiment, we observed nonlinear agglomeration behavior approaching stabilization in thermodynamically unstable bimodal colloidal systems in microgravity. Specifically, 2/9 (22%) of our samples showed definite nonlinear behavior, and an additional 2/9 (22%) samples resembled similar behavior, but there was not enough transient data to be conclusive. Considering the lack of variation in final growth rates across multiple nanoparticle concentrations, we present the possibility of transport-driven stabilization in dilute colloidal systems via the absence of buoyancy forces in microgravity. This experiment lays the groundwork for future study of bimodal and NPH systems aboard the ISS through particle tracking and study of transient effects immediately post mixing.

ACKOWLEDGMENTS

NASA EPSCoR (NNX14AN28A) "Influence of gravity on electrokinetic and electrochemical colloidal self-assembly for future materials"
ZIN-Technologies

AUTHOR DISCLOSURE STATEMENT

No competing financial interests exist.

REFERENCES

Ansari RR, Hovenac EA, Sankaran S, Koudelka JM, Weitz DA, Cipelletti L, Segre PN (1999) Physics of colloids in space experiment. Space Technology and Applications International Forum.

Asakura S, Oosawa F (1958) Interaction between particles suspended in solutions of macromolecules. *Journal of Polymer Science* **33**(126), 183–192. doi: 10.1002/pol.1958.1203312618

Bakhshandeh A, Frydel D, Levin Y (2020) Charge regulation of colloidal particles in aqueous solutions. *Physical Chemistry Chemical Physics* **22**(42), 24712–24728. doi: 10.1039/d0cp03633a

Bradski G (2000) The OpenCV Library. *Dr. Dobb's Journal of Software Tools*.

Cecil A (2021a) *Colloidspy*. In (Version 2021.2) Github. Available at: https://github.com/UofL-ACE/colloidspy

Cecil AJ (2021b) *Image Analysis of Charged Bimodal Colloidal Systems in Microgravity* (Publication Number 3437) University of Louisville]. Electronic Theses and Dissertations. Available at: https://ir.library.louisville.edu/etd/3437

Chatterjee AP, Schweizer KS (1998a) Correlation effects in dilute particle-polymer mixtures. *The Journal of Chemical Physics* **109**(23), 10477–10488. doi: 10.1063/1.477730

Chatterjee AP, Schweizer KS (1998b) Microscopic theory of polymer-mediated interactions between spherical particles. *The Journal of Chemical Physics* **109**(23), 10464–10476. doi: 10.1063/1.477729

Chu XL, Nikolov AD, Wasan DT (1996) Effects of particle size and polydispersity on the depletion and structural forces in colloidal dispersions. *Langmuir* **12**(21), 5004–5010. doi: 10.1021/la960359u

Contributor biographical information. Available at: http://www.loc.gov/catdir/enhancements/fy0838/2008447709-b.html

Grządka E (2015) Factors influencing the stability of the polysucrose/alumina system. *Colloid and Polymer Science* **293**(10), 2845–2853. doi: 10.1007/s00396-015-3677-6

Harris CR, Millman KJ, van der Walt SJ, Gommers R, Virtanen P, Cournapeau D, Wieser E, Taylor J, Berg S, Smith NJ, Kern R, Picus M, Hoyer S, van Kerkwijk MH, Brett M, Haldane A, del Río JF, Wiebe M, Peterson P, Gérard-Marchant P, Sheppard K, Reddy T, Weckesser W, Abbasi H, Gohlke C, Oliphant TE (2020) Array programming with NumPy. *Nature* **585**(7825), 357–362. doi: 10.1038/s41586-020-2649-2

Hiemenz PC (1972) The role of van der Waals forces in surface and colloid chemistry. *Journal of Chemical Education* **49**(3), 164. doi: 10.1021/ed049p164

Hunter RJ, Ottewill RH, Rowell RL (2013) *Zeta Potential in Colloid Science: Principles and Applications*. Elsevier Science. Available at: https://books.google.com/books?id=9I3-BAAAQBAJ

Israelachvili JN (2011) *Intermolecular and Surface Forces,* 3rd Edn. Academic Press.

Kontogeorgis GM, Kiil S (2016) Foams. In *Introduction to Applied Colloid and Surface Chemistry.* pp. 367. Wiley.

Kumar A, Dixit CK (2017) 3 – Methods for characterization of nanoparticles. In *Advances in Nanomedicine for the Delivery of Therapeutic Nucleic Acids,* S. Nimesh, R. Chandra, and N. Gupta (eds), pp. 43–58. Woodhead Publishing. doi: 10.1016/B978-0-08-100557-6.00003-1

Lant CT, Resnick A (2000) Multi-function Light Microscopy Module for the International Space Station. Space Technology and Applications International Forum.

Lewis JA (2000) Colloidal processing of ceramics. *Journal of the American Ceramic Society* **83**(10), 2341–2359.

Liu J, Shih WY, Kikuchi R, Aksay IA (1991) Clustering of binary colloidal suspensions: theory. *Journal of Colloid and Interface Science* **142**(2), 369–377. doi: 10.1016/0021-9797(91)90067-i

Lyklema J (2000) *Fundamentals of Interface and Colloid Science*. Academic Press. Publisher description. Available at: http://www.loc.gov/catdir/description/els031/00101585.html

McKinney W (2010) Data Structures for Statistical Computing in Python.

Mo S, Shao X, Chen Y, Cheng Z (2016) Increasing entropy for colloidal stabilization. *Scientific Reports* **6**(1), 36836. doi: 10.1038/srep36836

Moradi MWG, Williams, SJ, King B, Lee J (2017) Depletion in complex fluids with a bimodal particle size distribution under microgravity. *ASGSR 33rd Annual Meeting*, Seattle, WA.

Moradi M, He Q, Willing GA (2019a) Tuning the stabilization mechanism of nanoparticle-regulated complex fluids. *Colloids and Surfaces A: Physicochemical and Engineering Aspects* **577**, 532–540. doi: 10.1016/j.colsurfa.2019.06.021

Moradi M, Woods BM, Rathnayake H, Williams SJ, Willing GA (2019b) Effect of functionalization on the properties of silsesquioxane: a comparison to silica. *Colloid and Polymer Science* **297**(5), 697–704. doi: 10.1007/s00396-019-04489-3

Ninham BW, Parsegian VA (1971) Electrostatic potential between surfaces bearing ionizable groups in ionic equilibrium with physiologic saline solution. *Journal of Theoretical Biology* **31**(3), 405–428. doi: 10.1016/0022-5193(71)90019-1

Ottewill RH (1997) Stability of polymer colloids. pp. 31–48. Netherlands: Springer. doi: 10.1007/978-94-011-5512-0_3

Papadopulos F, Spinelli M, Valente S, Foroni L, Orrico C, Alviano F, Pasquinelli G (2007) Common tasks in microscopic and ultrastructural image analysis using ImageJ. *Ultrastructural Pathology* **31**(6), 401–407. doi: 10.1080/01913120701719189

Publisher description. Available at: http://www.loc.gov/catdir/enhancements/fy0712/2005025197-d.html

Python SF (2021). *Python*. In (Version 3.8).

Shah SA, Chen YL, Schweizer KS, Zukoski CF (2003) Phase behavior and concentration fluctuations in suspensions of hard spheres and nearly ideal polymers. *The Journal of Chemical Physics* **118**(7), 3350–3361. doi: 10.1063/1.1538602

Sinko PJ, Martin AN (2006) *Martin's Physical Pharmacy and Pharmaceutical Sciences: Physical Chemical and Biopharmaceutical Principles in the Pharmaceutical Sciences,* 5th Edn. Lippincott Williams & Wilkins. Table of contents. Available at: http://www.loc.gov/catdir/toc/ecip0518/2005025197.html

Swan JW, Vasquez PA, Whitson PA, Fincke EM, Wakata K, Magnus SH, Winne FD, Barratt MR, Agui JH, Green RD, Hall NR, Bohman DY, Bunnell CT, Gast AP, Furst EM (2012) Multi-scale kinetics of a field-directed colloidal phase transition. *Proceedings of the National Academy of Sciences of the United States of America* **109**(40), 16023–16028.

Table of contents only. Available at: http://www.loc.gov/catdir/enhancements/fy0838/2008447709-t.html

Tadros TF (2008) *Colloids in Cosmetics and Personal Care*. Wiley-VCH Verlag. Available at: http://www.loc.gov/catdir/enhancements/fy0838/2008447709-t.html

Tadros TF (2010) *Colloids in Paints*. Wiley-VCH Verlag. Publisher description. Available at: http://www.loc.gov/catdir/enhancements/fy0838/2008447709-d.html

Tohver V, Smay JE, Braem A, Braun PV, Lewis JA (2001) Nanoparticle halos: A new colloid stabilization mechanism. *Proceedings of the National Academy of Sciences of the United States of America* **98**(16), 8950–8954.

Van Der Walt S, Schönberger JL, Nunez-Iglesias J, Boulogne F, Warner JD, Yager N, Gouillart E, Yu, T (2014) Scikit-image: image processing in Python. *PeerJ* **2**, e453. doi: 10.7717/peerj.453

Veen SJ, Antoniuk O, Weber B, Potenza MAC, Mazzoni S, Schall P, Wegdam GH (2012) Colloidal aggregation in microgravity by critical Casimir forces. *Physical Review Letters* **109**, 248302.

Virtanen P, Gommers R, Oliphant TE, Haberland M, Reddy T, Cournapeau D, Burovski E, Peterson P, Weckesser W, Bright J, Van Der Walt SJ, Brett M, Wilson J, Millman KJ, Mayorov N, Nelson ARJ, Jones E, Kern R, Larson E, Carey CJ, Polat İ, Feng Y, Moore EW, Vanderplas J, Laxalde D, Perktold J, Cimrman R, Henriksen I, Quintero EA, Harris CR, Archibald AM, Ribeiro AH, Pedregosa F, Van Mulbregt P (2020) SciPy 1.0: fundamental algorithms for

scientific computing in Python. *Nature Methods* **17**(3), 261–272. doi: 10.1038/s41592-019-0686-2

Walz JY, Sharma A (1994) Effect of long range interactions on the depletion force between colloidal particles. *Journal of Colloid and Interface Science* **168**(2), 485–496. doi: 10.1006/jcis.1994.1446

Weight BM, Denton AR (2018) Structure and stability of charged colloid-nanoparticle mixtures. *The Journal of Chemical Physics* **148**(11), 114904. doi: 10.1063/1.5004443

Wiederseiner S, Andreini N, Epely-Chauvin G, Ancey C (2011) Refractive-index and density matching in concentrated particle suspensions: A review. *Experiments in Fluids* **50**, 1183-1206.

Yasrebi M, Shih WY, Aksay IA (1991) Clustering of binary colloidal suspensions: Experiment. *Journal of Colloid and Interface Science* **142**(2), 357–368. doi: 10.1016/0021-9797(91)90066-h